Suppression of antiferromagnetic order and orthorhombic distortion in superconducting $Ba(Fe_{0.961}Rh_{0.039})_2As_2$

A. Kreyssig, M. G. Kim, S. Nandi, D. K. Pratt, W. Tian, J. L. Zarestky, N. Ni, A. Thaler, S. L. Bud'ko, P. C. Canfield, R. J. McQueeney, and A. I. Goldman

Ames Laboratory, U.S. DOE and Department of Physics and Astronomy, Iowa State University, Ames, Iowa 50011, USA

(Received 24 February 2010; revised manuscript received 23 March 2010; published 12 April 2010)

Neutron-diffraction and high-resolution x-ray diffraction studies find that, similar to the closely related underdoped $Ba(Fe_{1-x}Co_x)_2As_2$ superconducting compounds, $Ba(Fe_{0.961}Rh_{0.039})_2As_2$ shows strong evidence of competition and coexistence between superconductivity and antiferromagnetic order below the superconducting transition, $T_c=14$ K. The transition temperatures for both the magnetic order and orthorhombic distortion are in excellent agreement with those inferred from resistivity measurements, and both order parameters manifest a distinct decrease in magnitude below T_c. These data suggest that the strong interaction between magnetism and superconductivity is a general feature of electron-doped $Ba(Fe_{1-x}TM_x)_2As_2$ superconductors (TM=transition metal).

DOI: 10.1103/PhysRevB.81.134512 PACS number(s): 74.70.Xa, 61.50.Ks, 75.30.Kz, 74.62.Bf

Recent systematic neutron- and x-ray diffraction studies of the underdoped $Ba(Fe_{1-x}Co_x)_2As_2$ superconductors have revealed several startling results regarding the interactions among structure, magnetism, and superconductivity. The undoped $AEFe_2As_2$ parent compounds (AE=Ba, Sr, or Ca) manifest simultaneous transitions from a high-temperature paramagnetic tetragonal phase to a low-temperature orthorhombic antiferromagnetic (AFM) structure.[1–4] Upon doping with Co for Fe in $Ba(Fe_{1-x}Co_x)_2As_2$,[5] however, both the structural (T_S) and antiferromagnetic order (T_N) transitions are suppressed to lower temperatures and split, with T_S slightly higher than T_N.[6–8] Several neutron and x-ray studies have clearly established that both the magnetic ordering and orthorhombic distortion are distinctly sensitive to superconductivity throughout the $Ba(Fe_{1-x}Co_x)_2As_2$ series.[8–12] At a given Co composition, as the sample temperature is reduced below T_c, there is a clear suppression of the magnetic order parameter and, in fact, reentrance into the paramagnetic phase is observed for a Co-doping concentration of $x=0.059$.[11] Similarly, the magnitude of the orthorhombic lattice distortion, as evidenced by high-resolution x-ray diffraction measurements of peak splitting in $Ba(Fe_{1-x}Co_x)_2As_2$, decreases below T_c and reentrance into the tetragonal structure was observed at Co-doping concentrations of $x=0.063$.[12] This striking behavior for $Ba(Fe_{1-x}Co_x)_2As_2$ is unprecedented and has been related to the strong coupling between superconductivity and magnetism[11] as well as an unusual magnetoelastic coupling in the form of emergent nematic order in the iron arsenides.[12–15]

This unusual behavior has not, until now, been reported for other doping species in the $AE(Fe_{1-x}TM_x)_2As_2$ family of compounds,[16–19] but is widely suspected. Studies of bulk thermodynamic and transport properties of $Ba(Fe_{1-x}TM_x)_2As_2$, for TM=Co, Ni, Cu, Rh, or Pd, have recently been reviewed in some detail[20] and noted that superconductivity appears when two conditions are satisfied: (i) the structural and magnetic phase transitions must be suppressed to sufficiently low temperatures while (ii) the number of additional electrons contributed by the doping falls within a specific window. These points are supported by, for example, the absence of superconductivity for Cu doping.[21] Nevertheless, the behavior of the structural and magnetic transitions for all doping species, in the underdoped regime, is quite similar to what has been found for the case of Co doping; both transitions are suppressed in temperature and split. It is important to establish, if the behavior of the magnetic and structural order parameters in the superconducting state also carries over to the other doping species since differences, such as steric effects or disorder, may also play a role.

Here we report on neutron-diffraction measurements and high-resolution x-ray diffraction measurements on $Ba(Fe_{0.961}Rh_{0.039})_2As_2$ that confirm the same unusual behavior of the magnetic and structural order parameters below T_c. This composition was chosen for a direct comparison with previous results on $Ba(Fe_{0.953}Co_{0.047})_2As_2$,[9] i.e., the structural, magnetic, and superconducting transition temperatures for $Ba(Fe_{0.953}Co_{0.047})_2As_2$ are $T_S=60$ K, $T_N=47$ K, and $T_c=17$ K, respectively, and are close to the corresponding transition temperatures, $T_S=59$ K, $T_N=54$ K, and $T_c=14$ K, for $Ba(Fe_{0.961}Rh_{0.039})_2As_2$.

Single crystals of $Ba(Fe_{0.961}Rh_{0.039})_2As_2$ were grown out of a FeAs self-flux using conventional high-temperature solution growth.[22] The compositions were measured at 18 positions on several samples of the used batch by wavelength-dispersive spectroscopy to determine the Rh-doping composition as $x=0.039\pm0.002$. The samples emerge from the flux as plates with the tetragonal **c** axis perpendicular to the plate. The particular sample used for the neutron and x-ray measurements (mass of 260 mg) is shown as inset of Fig. 1, and exhibited a sharp sample mosaic in both x-ray [Fig. 1(a)] and neutron [Fig. 1(b)] rocking scans, demonstrating excellent sample quality. Magnetization and temperature-dependent ac electrical resistance data ($f=16$ Hz, $I=3$ mA) were collected in a Quantum Design magnetic properties measurement system using a Linear Research LR700 resistance bridge for the latter. Electrical contact was made to the sample using Epotek H20E silver epoxy to attach Pt wires in a four-probe configuration. As shown in Figs. 2(a) and 2(b), both the magnetization and resistivity measurements show

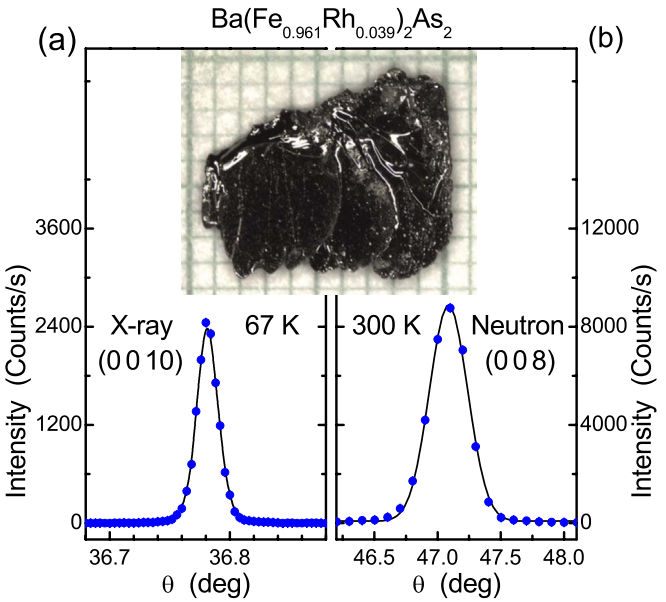

FIG. 1. (Color online) (a) X-ray and (b) neutron rocking curves of the $Ba(Fe_{0.961}Rh_{0.039})_2As_2$ sample investigated in this study. The picture shows the single crystal on a millimeter grid.

the onset of superconductivity in the sample at approximately 14 K, whereas the structural and magnetic transitions at higher temperatures are only weakly in evidence, but can be discerned in the derivative of the resistivity.

To elucidate the nature of the structural transition and its behavior below T_c, high-resolution single-crystal x-ray diffraction measurements were performed on a four-circle diffractometer using Cu $K\alpha 1$ radiation from a rotating anode x-ray source, selected by a germanium (1 1 1) monochromator. For these measurements, the platelike single crystal was attached to a flat copper sample holder on the cold finger of a closed-cycle displex refrigerator. The mosaicity of the $Ba(Fe_{0.961}Rh_{0.039})_2As_2$ single crystal was less than 0.02° deg full width at half maximum as measured by the rocking curve of the (0 0 10) reflection at room temperature [Fig. 1(a)]. The diffraction data were obtained as a function of temperature between room temperature and 10 K, the base temperature of the refrigerator. Figure 3(a) shows a subset of ($\xi\xi 0$) scans through the (1 1 10) reflection as the sample was cooled through $T_S=59$ K. The splitting of the peak below T_S is consistent with the structural transition, from space group $I4/mmm$ to $Fmmm$, with a distortion along the [1 1 0] direction. As the sample is cooled further, the orthorhombic splitting increases until $T_c=14$ K. Lowering the temperature below T_c results in a decrease in the orthorhombic distortion consistent with what was previously observed for $Ba(Fe_{1-x}Co_x)_2As_2$.[12] The extrapolated value $(1.4\pm0.1)\times10^{-3}$ for $T=0$ K is also the same, within experimental error, as observed in $Ba(Fe_{0.953}Co_{0.047})_2As_2$.[12]

Neutron-diffraction measurements were performed on the HB1A diffractometer at the High Flux Isotope Reactor at Oak Ridge National Laboratory using a sample with a mass of 260 mg and a resolution limited crystal mosaic (<0.3° full width at half maximum). The experimental configuration was 48′-48′-40′-68′ with fixed incident neutron energy of 14.7 meV, and two pyrolytic graphite filters for the elimination of higher harmonics in the incident beam. The sample was aligned in the (H H L) scattering plane and mounted in a closed-cycle refrigerator.

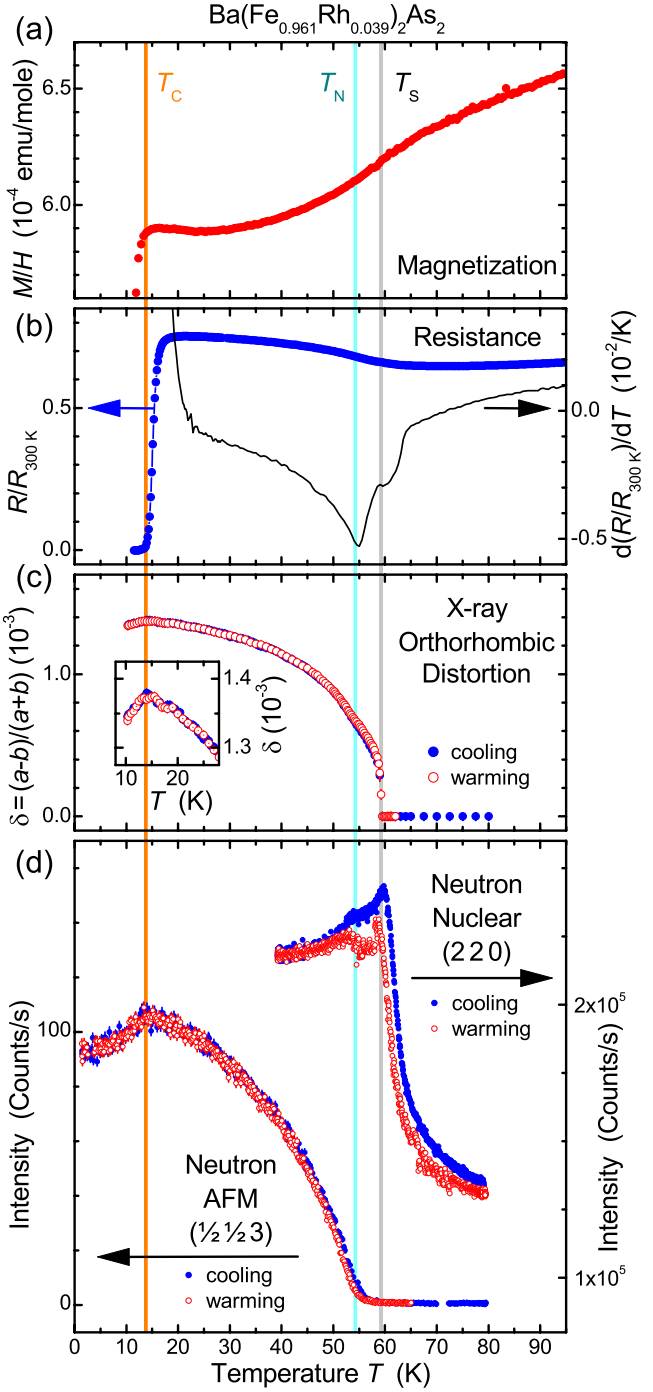

FIG. 2. (Color online) (a) Measured magnetization of $Ba(Fe_{0.961}Rh_{0.039})_2As_2$ showing the superconducting transition at $T_c=14$ K. (b) Resistance (points) and its derivative (line) showing the signature of T_S, T_N, and T_c. (c) Orthorhombic distortion measured as a function of temperature on cooling and warming. The inset shows an expanded region close to T_c to emphasize the decrease in the orthorhombicity in the superconducting state. (d) Intensity of the nuclear (2 2 0) reflection as a function of temperature close to T_S on cooling and warming, and the intensity of the (1/2 1/2 3) magnetic reflection on cooling and warming.

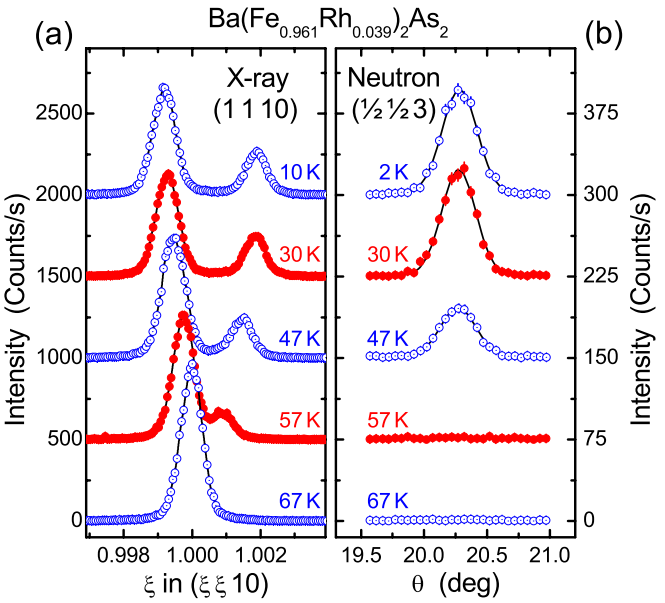

FIG. 3. (Color online) Transverse scans through (a) the (1 1 10) charge reflection and (b) the (1/2 1/2 3) magnetic reflection demonstrating the transition between the tetragonal and orthorhombic structures and the onset of AFM order, respectively.

Even though the instrumental resolution of the neutron spectrometer was insufficient to resolve the splitting of nuclear peaks at the tetragonal-to-orthorhombic transition, the structural distortion can be discerned through the behavior of the nuclear peaks in the vicinity of T_S. Figure 2(d) shows the evolution of the integrated intensity of the (2 2 0) nuclear reflection with temperature. We find that as the temperature decreases below approximately 65 K, the intensity of the (2 2 0) reflection increases sharply and peaks at 59 K. The peak is observed at the same transition temperature, T_S, determined in the high-resolution x-ray study. The increase in intensity of the (2 2 0) reflection arises from the extinction release that occurs due to stress, strain, and domain formation related to the orthorhombic distortion. This effect is strongest at the transition because the fluctuations are strongest, leading to a maximum in local stress and strain which decreases above and below the transition. The observation of measurable extinction release at temperatures well above T_S indicates the presence of significant structural fluctuations related to the orthorhombic distortion. Indeed, this effect sets in at roughly the same temperature where deviations of transport properties [see Fig. 2(b)] from their high-temperature behavior are first observed, pointing to significant electron scattering by the structural fluctuations. Below the structural transition, the orthorhombic lattice distortion leads to twin domains that grow in size with decreasing temperature. The impact of these twin domains on the nuclear (2 2 0) reflection is demonstrated by the occurrence of an additional distinct feature in the temperature dependence of the intensity at T_N=54 K. At this temperature, due to strong magnetoelastic coupling,[12,15] the domain structure changes again at the onset of magnetic order. The high quality of the sample is, again, evidenced by the relatively strong extinction release at the structural transition and the fact that even the mild change in extinction associated with the magnetic transition is easily observed.

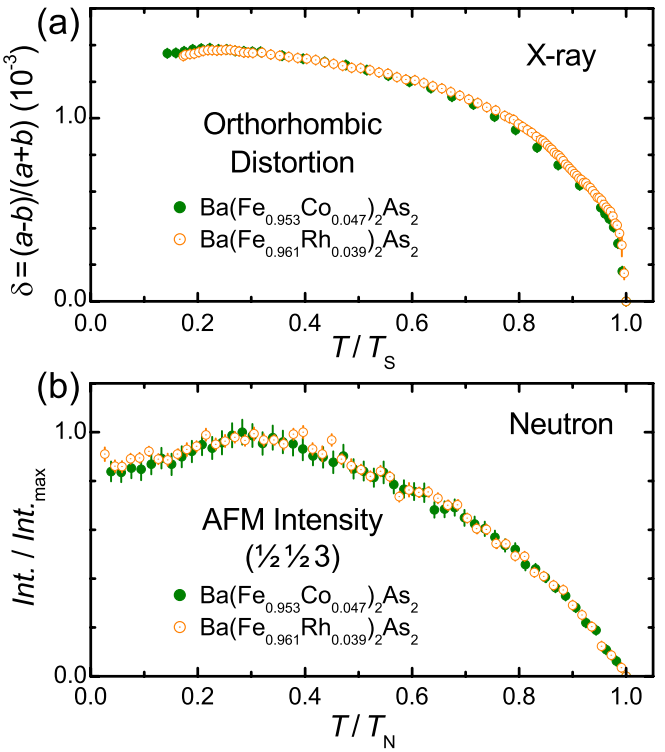

FIG. 4. (Color online) (a) Measured orthorhombic distortions for $Ba(Fe_{0.961}Rh_{0.039})_2As_2$ and $Ba(Fe_{0.953}Co_{0.047})_2As_2$ as function of reduced temperature T/T_S. (b) Integrated intensity of the (1/2 1/2 3) magnetic reflections for $Ba(Fe_{0.961}Rh_{0.039})_2As_2$ and $Ba(Fe_{0.953}Co_{0.047})_2As_2$ normalized to their maximum value at T_c plotted as function of reduced temperature T/T_N.

The x-ray results in Fig. 2(c) and the neutron-diffraction extinction release profile in Fig. 2(d) allow us to refine the assignment of the structural transition in resistivity (R) measurements. In previous work,[9,22] T_S was estimated from the first deviation in dR/dT from its high-temperature behavior. Here, we see that T_S is most appropriately associated with the first minimum in dR/dT which falls at a slightly lower temperature.

Magnetic reflections were observed at $\mathbf{Q_{AFM}}$=(1/2 1/2 L) positions with L odd. Scans at several representative temperatures are shown in Fig. 3(b). From the data at 57 K we see that the AFM order sets in at lower temperatures than the orthorhombic distortion illustrated by the finite splitting of the (1 1 10) reflection in Fig. 3(a) without the appearance of a magnetic (1/2 1/2 L) reflection in Fig. 3(b). The magnetic propagation vector is identical to that for $BaFe_2As_2$ and the $Ba(Fe_{1-x}Co_x)_2As_2$ compounds, indicating that the magnetic structure is the same AFM "stripe" structure observed for all of the AFM ordered iron arsenides. Analysis of the intensity ratios of different AFM reflections at selected temperatures confirms that the moment direction is the same along the elongated orthorhombic **a** direction.

Figure 2(d) shows the magnetic order parameter obtained from the intensity measured at $\mathbf{Q_{AFM}}$=(1/2 1/2 3) as function of temperature for $Ba(Fe_{0.961}Rh_{0.039})_2As_2$. Above T_N =54 K, no scattering is observed at $\mathbf{Q_{AFM}}$, but increases smoothly below T_N. Furthermore, lowering the temperature below T_c=14 K results in a decrease in the magnetic order

parameter in the same manner, and nearly the same magnitude, as observed for $Ba(Fe_{0.953}Co_{0.047})_2As_2$, indicating that the strong coupling between superconductivity and magnetism is not exclusive to $Ba(Fe_{1-x}Co_x)_2As_2$ compounds. Using the measured mass of the sample and assuming that the entire sample contributes to the scattering at $\mathbf{Q_{AFM}}=(1/2\ 1/2\ 3)$, the magnetic scattering data were normalized using the parent $BaFe_2As_2$ compound as a standard through the process described in Refs. 9 and 11. The extrapolated ordered moment at zero temperature was determined to be $(0.37\pm0.1)\mu_B$, somewhat larger than the value $(0.25\pm0.1)\mu_B$ determined for $Ba(Fe_{0.953}Co_{0.047})_2As_2$,[9,11] but well below the value $(0.87\pm0.1)\mu_B$ for the parent $BaFe_2As_2$ compound.[1]

Taken together, these data clearly show that the suppression of the magnetic and structural order parameters previously observed in $Ba(Fe_{1-x}Co_x)_2As_2$ in the superconducting regime are also observed in $Ba(Fe_{0.961}Rh_{0.039})_2As_2$. This point is most clearly made in Fig. 4, which plots the magnitude of the orthorhombic distortion [Fig. 4(a)] and the intensity of the (1/2 1/2 3) magnetic diffraction peaks [Fig. 4(b)] for both $Ba(Fe_{0.953}Co_{0.047})_2As_2$ and $Ba(Fe_{0.961}Rh_{0.039})_2As_2$. Here we have plotted the data in terms of the reduced temperature scale T/T_S and T/T_N, respectively, to emphasize the close similarity in the behavior of these compounds manifested in: (i) similar temperature dependence for the magnetic and structural order parameters; (ii) the similar absolute value of the distortion and; (iii) the similar qualitative and quantitative effects of superconductivity on both order parameters. These results suggest that the strong interaction between magnetism, structure, and superconductivity is a general feature of electron-doped $BaFe_2As_2$ superconductors.

Note added. Recently, a neutron-scattering study[23] in $Ba(Fe_{1-x}Ni_x)_2As_2$ compounds has appeared that shows a suppression of the AFM signal below T_c for an underdoped sample confirming our previous results[9,11] and the present work.

We thank A. Kracher for performing the WDS measurements. This work was supported by the U.S. Department of Energy, Office of Basic Energy Science, Division of Materials Sciences and Engineering. The research was performed at the Ames Laboratory. Ames Laboratory is operated for the U.S. Department of Energy by Iowa State University under Contract No. DE-AC02-07CH11358. Work at Oak Ridge National Laboratory is supported by U.S. Department of Energy, Office of Basic Energy Sciences, Scientific User Facilities Division.

[1] Q. Huang, Y. Qiu, W. Bao, M. A. Green, J. W. Lynn, Y. C. Gasparovic, T. Wu, G. Wu, and X. H. Chen, Phys. Rev. Lett. **101**, 257003 (2008).
[2] A. Jesche, N. Caroca-Canales, H. Rosner, H. Borrmann, A. Ormeci, D. Kasinathan, H. H. Klauss, H. Luetkens, R. Khasanov, A. Amato, A. Hoser, K. Kaneko, C. Krellner, and C. Geibel, Phys. Rev. B **78**, 180504(R) (2008).
[3] A. I. Goldman, D. N. Argyriou, B. Ouladdiaf, T. Chatterji, A. Kreyssig, S. Nandi, N. Ni, S. L. Bud'ko, P. C. Canfield, and R. J. McQueeney, Phys. Rev. B **78**, 100506(R) (2008).
[4] N. Ni, S. Nandi, A. Kreyssig, A. I. Goldman, E. D. Mun, S. L. Bud'ko, and P. C. Canfield, Phys. Rev. B **78**, 014523 (2008).
[5] A. S. Sefat, R. Jin, M. A. McGuire, B. C. Sales, D. J. Singh, and D. Mandrus, Phys. Rev. Lett. **101**, 117004 (2008).
[6] N. Ni, M. E. Tillman, J.-Q. Yan, A. Kracher, S. T. Hannahs, S. L. Bud'ko, and P. C. Canfield, Phys. Rev. B **78**, 214515 (2008).
[7] J.-H. Chu, J. G. Analytis, C. Kucharczyk, and I. R. Fisher, Phys. Rev. B **79**, 014506 (2009).
[8] C. Lester, J.-H. Chu, J. G. Analytis, S. C. Capelli, A. S. Erickson, C. L. Condron, M. F. Toney, I. R. Fisher, and S. M. Hayden, Phys. Rev. B **79**, 144523 (2009).
[9] D. K. Pratt, W. Tian, A. Kreyssig, J. L. Zarestky, S. Nandi, N. Ni, S. L. Bud'ko, P. C. Canfield, A. I. Goldman, and R. J. McQueeney, Phys. Rev. Lett. **103**, 087001 (2009).
[10] A. D. Christianson, M. D. Lumsden, S. E. Nagler, G. J. MacDougall, M. A. McGuire, A. S. Sefat, R. Jin, B. C. Sales, and D. Mandrus, Phys. Rev. Lett. **103**, 087002 (2009).
[11] R. M. Fernandes, D. K. Pratt, W. Tian, J. Zarestky, A. Kreyssig, S. Nandi, M. G. Kim, A. Thaler, N. Ni, P. C. Canfield, R. J. McQueeney, J. Schmalian, and A. I. Goldman, Phys. Rev. B **81**, 140501(R) (2010).
[12] S. Nandi, M. G. Kim, A. Kreyssig, R. M. Fernandes, D. K. Pratt, A. Thaler, N. Ni, S. L. Bud'ko, P. C. Canfield, J. Schmalian, R. J. McQueeney, and A. I. Goldman, Phys. Rev. Lett. **104**, 057006 (2010).
[13] C. Fang, H. Yao, W.-F. Tsai, J. P. Hu, and S. A. Kivelson, Phys. Rev. B **77**, 224509 (2008).
[14] C. Xu, M. Müller, and S. Sachdev, Phys. Rev. B **78**, 020501(R) (2008).
[15] R. M. Fernandes, L. H. VanBebber, S. Bhattacharya, P. Chandra, V. Keppens, D. Mandrus, M. A. McGuire, B. C. Sales, A. S. Sefat, and J. Schmalian, arXiv:0911.3084 (unpublished).
[16] L. J. Li, Y. K. Luo, Q. B. Wang, H. Chen, Z. Ren, Q. Tao, Y. K. Li, X. Lin, M. He, Z. W. Zhu, G. H. Cao, and Z. A. Xu, New J. Phys. **11**, 025008 (2009).
[17] S. Sharma, A. Bharathi, S. Chandra, R. Reddy, S. Paulraj, A. T. Satya, V. S. Sastry, A. Gupta, and C. S. Sundar, arXiv:0902.2728 (unpublished).
[18] A. Leithe-Jasper, W. Schnelle, C. Geibel, and H. Rosner, Phys. Rev. Lett. **101**, 207004 (2008).
[19] F. Han, X. Zhu, P. Cheng, G. Mu, Y. Jia, L. Fang, Y. Wang, H. Luo, B. Zeng, B. Shen, L. Shan, C. Ren, and H.-H. Wen, Phys. Rev. B **80**, 024506 (2009).
[20] P. C. Canfield and S. L. Bud'ko, arXiv:1002.0858, Condens. Matter Phys. (to be published).
[21] P. C. Canfield, S. L. Bud'ko, N. Ni, J. Q. Yan, and A. Kracher, Phys. Rev. B **80**, 060501(R) (2009).
[22] N. Ni, A. Thaler, A. Kracher, J. Q. Yan, S. L. Bud'ko, and P. C. Canfield, Phys. Rev. B **80**, 024511 (2009).
[23] M. Wang, H. Luo, J. Zhao, C. Zhang, M. Wang, K. Marty, S. Chi, J. W. Lynn, A. Schneidewind, S. Li, and P. Dai, arXiv:1002.3133 (unpublished).